Morphologic Analysis in Pathologic Myopia Using High-Penetration Optical Coherence Tomography

Ichiro Maruko,[1] *Tomohiro Iida,*[1,2] *Yukinori Sugano,*[1] *Hiroshi Oyamada,*[1] *Masahiro Akiba,*[3] *and Tetsuju Sekiryu*[1]

Purpose. We evaluated retrospectively the morphologic choroidal and scleral characteristics in eyes with pathologic myopia using high-penetration optical coherence tomography (HP-OCT) or swept-source OCT (SS-OCT).

Methods. The subfoveal choroidal and scleral thicknesses were measured using the prototype HP-OCT with a 1060 nm light source. We also measured the scleral thickness 3 mm superior, inferior, nasal, and temporal to the fovea on the horizontal and vertical OCT sections. The axial length (AL) in all eyes was measured using optical biometry.

Results. We examined 58 eyes of 35 patients (7 men and 28 women, mean age 65.5 years) with an AL exceeding 26.5 mm. The mean AL was 29.0 ± 1.4 mm. The full-thickness choroid and sclera were visualized in all eyes. The mean subfoveal choroidal and scleral thicknesses were 52 ± 38 and 335 ± 130 μm, respectively. The mean scleral thicknesses 3 mm superior, inferior, nasal, and temporal to the fovea were 266 ± 78 (n = 57), 259 ± 72 (n = 56), 324 ± 109 (n = 39), and 253 ± 79 (n = 58) μm, respectively. The subfoveal sclera was thicker than 3 mm outside the fovea ($P < 0.05$, for each comparison).

Conclusions. The full-thickness choroid and sclera in all eyes with pathologic myopia were visualized using a prototype HP-OCT. The subfoveal sclera was thicker than 3 mm outside the fovea. HP-OCT is a useful tool for morphologic analyses of pathologic myopia. (*Invest Ophthalmol Vis Sci.* 2012;53:3834–3838) DOI:10.1167/iovs.12-9811

Although pathologic myopia is thought to induce ocular global stretching at the posterior pole, the mechanisms of the morphologic changes are not fully understood. In cadaver eyes without high myopia, the scleral thickness was approximately 0.9 mm at the subfoveal area and approximately 1.0 mm around the peripapillary area.[1] However, the sclera in highly myopic eyes might have become thinner due to global expansion accompanied by a long axial length (AL).

Spectral-domain optical coherence tomography (SD-OCT) can detect noninvasively morphologic changes at the posterior pole in a number of macular diseases. Recent OCT studies have reported choroidal thickness measurements using enhanced depth imaging (EDI) OCT[2–7] with conventional SD-OCT or high-penetration (HP) OCT[8–11] with a 1 μm wavelength light source applied by swept source (SS) system. Fujiwara et al. reported that the choroid in highly myopic eyes was much thinner than in normal eyes.[3] However, few studies of the sclera have been published. Ohno-Matsui et al. reported on the subarachnoid space and sclera around the optic nerve using HP-OCT.[12] Using EDI-OCT, we recently measured the scleral thickness in dome-shaped maculas associated with highly myopic eyes,[13] and using HP-OCT, we observed the sclera in a patient with tilted disc syndrome.[14]

In our current study, we used HP-OCT to evaluate the morphologic choroidal and scleral characteristics at the posterior pole in eyes with pathologic myopia.

Methods

Our retrospective study followed the tenets of the Declaration of Helsinki. The institutional review board at Fukushima Medical University School of Medicine approved this study, which included OCT observation of eyes with macular and retinal disorders, observational study of age-related macular degeneration and similar disorders (including pathologic myopia), and use of the prototype HP-OCT not available commercially (Fig. 1).

Our study included highly myopic eyes with an AL exceeding 26.5 mm measured by non-contact optical biometry. Although the spherical equivalent refractive error was helpful to enroll the cases, we did not include it in the current study because it is possible to underestimate the spherical equivalent after cataract surgery. The clinical examinations to diagnose pathologic myopia included measurement of the best-corrected visual acuity (BCVA), slit-lamp biomicroscopy with a contact or non-contact lens, and indirect ophthalmoscopy. The BCVA was measured with a Japanese standard decimal visual chart, and the visual acuity (VA) levels were converted to the logarithm of the minimum angle of resolution (logMAR) scale for statistical analysis. Fundus color photographs were taken of all eyes. Digital fluorescein angiography (FA) and indocyanine green angiography (ICGA, TRC-50IX/IMAGEnet H1024 system; Topcon, Tokyo, Japan) were performed in eyes with a subretinal hemorrhage or suspicious choroidal neovascularization (CNV). We measured the spherical equivalent refractive error using autorefractometry (Nidek, Gamagori, Japan) and the AL using the IOLMaster (Carl Zeiss Meditec, Dublin, CA).

All eyes were examined with the prototype HP-OCT or SS-OCT with a 1060 nm wavelength (Topcon). This instrument can average up to 50 images to improve the signal-to-noise ratio, and enhance the choroid and sclera by moving the reference mirror to adjust the focus, similar to EDI-OCT when positioned close to the eye. If a convex elevation of the macula was seen using HP-OCT, we diagnosed a dome-shaped macula.[13] The choroid was defined as the area between the outer retinal pigment epithelium surface and the inner scleral surface. OCT visualized the sclera as hyperreflective tissue. We recognized the full-thickness sclera by visualizing an area of no reflectivity under the sclera. The absence of any reflection from the dark area behind the

From the [1]Department of Ophthalmology, Fukushima Medical University School of Medicine, Fukushima, Japan; the [2]Department of Ophthalmology, Tokyo Women's Medical University School of Medicine, Tokyo, Japan; and [3]Topcon Corp., Tokyo, Japan.

Submitted for publication March 7, 2012; revised April 24, 2012; accepted May 7, 2012.

Disclosure: **I. Maruko**, None; **T. Iida**, None; **Y. Sugano**, None; **H. Oyamada**, None; **M. Akiba**, Topcon Corp. (E); **T. Sekiryu**, None

Corresponding author: Ichiro Maruko, Department of Ophthalmology, Fukushima Medical University School of Medicine, 1 Hikarigaoka, Fukushima, Japan; imaruko@fmu.ac.jp.

Investigative Ophthalmology & Visual Science, June 2012, Vol. 53, No. 7

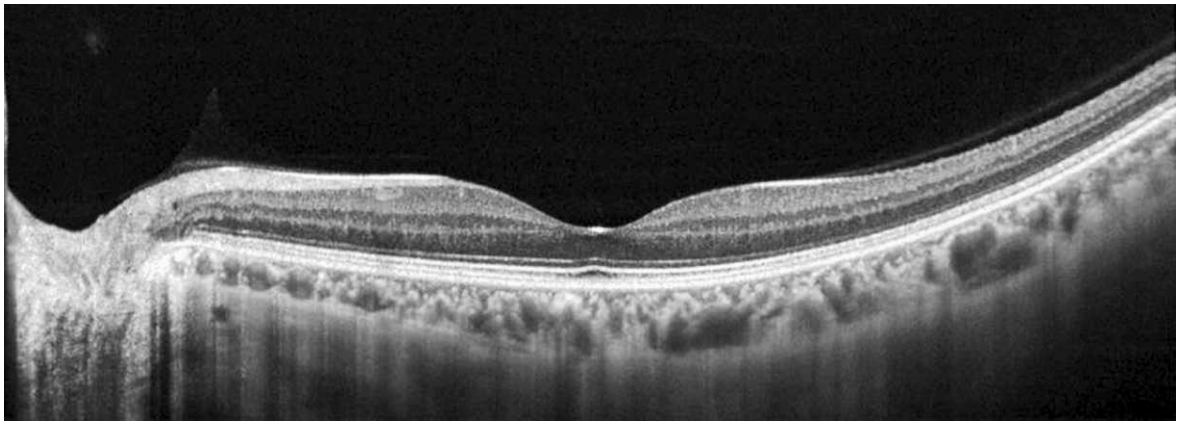

Figure 1. Normal horizontal scan image on HP-OCT. Retinal layers, choroid, and scleral choroidal interface were visualized beautifully.

scleral hyperreflectivity was considered to be the presence of other structures, including the connective tissues, vessels, muscles, or orbital fat. The standard scanning length was 12 mm. The central retinal thickness, and subfoveal choroidal and scleral thicknesses were measured using the caliper tool in the OCT software. We also measured the scleral thicknesses 3 mm superior, inferior, nasal, and temporal to the fovea on the horizontal and vertical OCT scans passing through the fovea (Figs. 2, 3).

The reported measurements obtained from the OCT images represented the average measurements examined by three individuals (IM, YS, HO). The VAs are expressed as the decimal and logMAR equivalents. The standard Snellen VA values also were recorded. The results of the measurement of the choroidal and scleral thicknesses were analyzed using the Wilcoxon signed-rank test between paired groups and the Mann-Whitney *U* test between unpaired groups. $P < 0.05$ was considered significant. Multiple linear regression analysis was performed to evaluate the correlation between the scleral thickness and other factors, including age, AL, and choroidal thickness.

Results

We examined 58 eyes of 35 patients (7 men and 28 women, mean age 65.5 years) with an AL exceeding 26.5 mm using HP-OCT. The mean AL was 29.0 ± 1.4 mm (range 26.6–33.2 mm). The full-thickness choroid and sclera were visualized in all eyes. The mean BCVA was 0.62 (20/32 Snellen, 0.34 logMAR). The mean spherical equivalent was −12.8 ± 3.6 diopters excluding the 24 eyes that had undergone cataract surgery. CNV was observed in 10 eyes as demarcated hyperfluorescence on FA and ICGA. All eyes had the myopic conus at the peripapillary area. Posterior staphyloma was identified retrospectively in 22 (37.9%) eyes, which were confirmed by the data in the medical records and fundus photography. A dome-shaped macula was diagnosed in seven eyes. Only one eye had a macular hole. Figures 2 and 3 show representative cases in an eye with CNV and an eye with a dome-shaped macula.

In all 58 eyes, the mean central retinal thickness and subfoveal choroidal/scleral thicknesses were 206 ± 92 (range

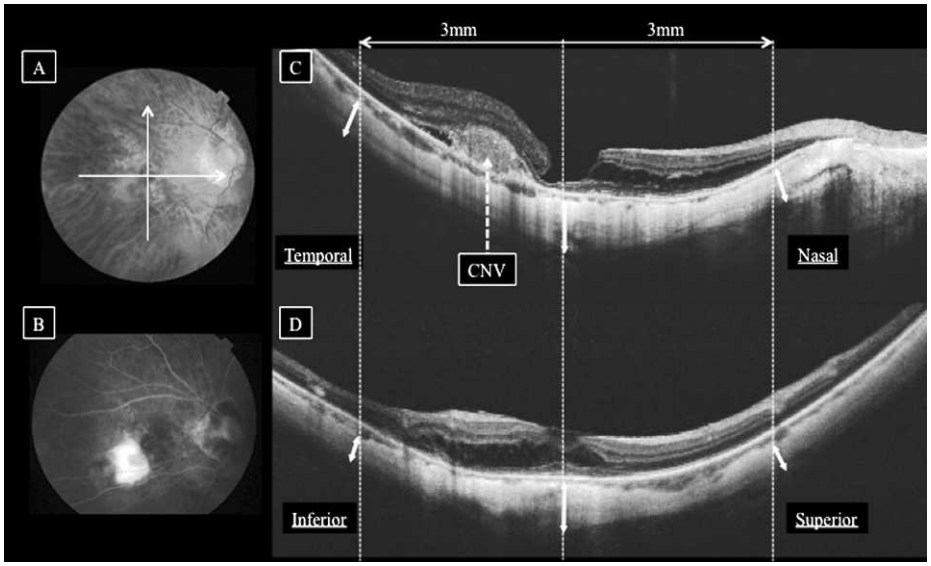

Figure 2. An 81-year-old woman has CNV in the right eye. The BCVA is 0.50 (20/40 Snellen, 0.30 logMAR). The AL is 28.5 mm. (**A**) A gray-scale fundus photograph of the right eye shows a whitish lesion inferotemporal to the fovea. The *white arrows* indicate the horizontal (**C**) and vertical (**D**) scan lines on OCT. (**B**) FA of the right eye shows hyperfluorescence inferotemporal to the fovea. (**C**, **D**) The dotted lines indicate the full-thickness choroid and sclera seen at the subfoveal area, and 3 mm superior, inferior, nasal, and temporal to the fovea. A horizontal HP-OCT image (**C**) shows the hyperreflective tissue as a choroidal neovascularization temporal to the fovea (*white-dotted arrow*). The scleral thicknesses are measured at each *white-thick arrow*.

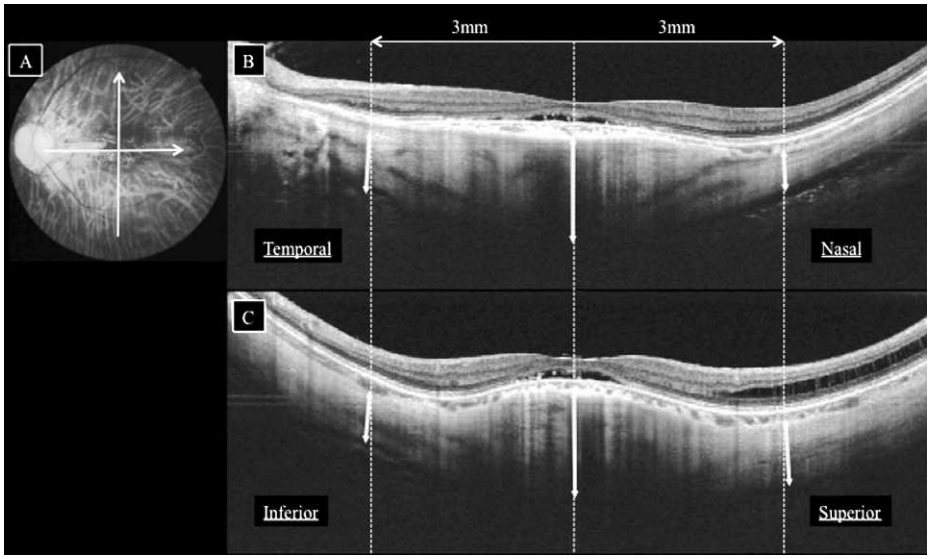

Figure 3. A 56-year-old woman has a dome-shaped macula in the right eye. The BCVA is 0.40 (20/50 Snellen, 0.40 logMAR). The AL is 27.2 mm. (**A**) A gray-scale fundus photograph of the left eye shows atrophic change at the fovea. The *white arrows* indicate the horizontal (**B**) and vertical (**C**) scan lines on OCT. (**B**, **C**) The *dotted lines* indicate the full-thickness choroid and sclera at the subfoveal area, and 3 mm superior, inferior, nasal, and temporal to the fovea. Horizontal and vertical HP-OCT images show the thickened sclera and a serous retinal detachment at the subfoveal area. The scleral thicknesses are measured at each *white-thick arrow*.

0–578), 52 ± 38 (range 11–167), and 335 ± 130 (range 167–735) μm, respectively. The mean scleral thicknesses 3 mm superior, inferior, nasal, and temporal to the fovea were 266 ± 78 ($n = 57$), 259 ± 72 ($n = 56$), 324 ± 109 ($n = 39$), and 253 ± 79 ($n = 58$) μm, respectively. The mean subfoveal sclera was thicker than 3 mm outside the fovea ($P < 0.05$, for each comparison). The scleral thickness 3 mm nasal to the fovea could not be measured even in all eyes because of the artifacts due to the large myopic conus.

Table 1 shows the results in eyes with CNV, posterior staphyloma, and a dome-shaped macula. The scleral thickness at some areas except for the subfoveal area could not be measured in several eyes due to missing data. The mean subfoveal scleral thicknesses in eyes with and without CNV were 333 ± 57 and 336 ± 141 μm, respectively; the difference did not reach significance. The mean subfoveal scleral thickness in eyes with posterior staphyloma was 294 ± 92 μm, which was significantly thinner than 362 ± 146 μm without posterior staphyloma ($P < 0.01$). The differences in the mean subfoveal choroidal thicknesses in eyes with and without posterior staphyloma also were significant (32 ± 18 and 63 ± 42 μm, respectively; $P < 0.01$).

As reported previously,[13] using EDI-OCT, the mean subfoveal sclera in eyes with a dome-shaped macula was significantly thicker than in eyes without an elevated macula (559 ± 167 vs. 305 ± 90 μm, $P < 0.01$). The mean scleral thicknesses 3 mm superior, inferior, nasal, and temporal to the fovea in seven eyes with a dome-shaped macula were 322 ± 109, 296 ± 102, 407 ± 175, and 284 ± 106 μm, respectively. The subfoveal sclera was significantly thicker than 3 mm outside of the fovea in eyes with a dome-shaped macula ($P < 0.01$, for all comparisons). However, the mean scleral thicknesses 3 mm superior, inferior, nasal, and temporal to the fovea without a dome-shaped macula were 258 ± 71 ($n = 50$), 254 ± 66 ($n = 49$), 306 ± 83 ($n = 32$), and 249 ± 75 ($n = 51$) μm, respectively. The mean subfoveal sclera was thicker than that 3 mm outside of the fovea ($P < 0.01$, for all comparisons), except 3 mm nasal to the fovea ($P = 0.83$).

The subfoveal choroidal and scleral thicknesses were weakly inversely correlated with age (Figs. 4A, 4B) and AL (Figs. 4C, 4D). We found a weak correlation between the subfoveal choroidal and scleral thicknesses (Fig. 4E). Table 2 shows the results of multiple linear regression analysis of the mean subfoveal scleral thickness. The multiple regression

Table 1. Central Retinal Thickness, Subfoveal Thickness, and Scleral Thickness in Eyes with Pathologic Myopia

Eyes	No. Eyes	Central Retinal Thickness (μm)	Subfoveal Choroidal Thickness (μm)	Scleral Thickness (μm)				
				Subfovea ($n = 58$)	Superior ($n = 57$)	Inferior ($n = 56$)	Nasal ($n = 39$)	Temporal ($n = 58$)
All eyes	58	206 ± 92	52 ± 38	335 ± 130	266 ± 78	259 ± 72	324 ± 109	253 ± 79
CNV (+)	10	207 ± 103	50 ± 32	333 ± 57	263 ± 39	254 ± 51	306 ± 89 (6)	234 ± 60
CNV (-)	48	206 ± 91	52 ± 39	336 ± 141	266 ± 85 (47)	260 ± 76 (46)	328 ± 113 (33)	257 ± 83
Staphyloma (+)	22	223 ± 116	32 ± 18*	294 ± 92*	230 ± 67 (21)	235 ± 55	279 ± 88 (13)	229 ± 77
Staphyloma (-)	36	195 ± 76	63 ± 42*	362 ± 146*	287 ± 79	275 ± 79 (34)	347 ± 113 (26)	268 ± 79
Dome-shaped macula (+)	7	211 ± 35	66 ± 41	559 ± 167*	322 ± 109	296 ± 102	407 ± 175	284 ± 106
Dome-shaped macula (-)	51	200 ± 88	52 ± 39	305 ± 90*	258 ± 71 (50)	254 ± 66 (49)	306 ± 83 (32)	249 ± 75 (51)

The scleral thickness was measured at the subfoveal area, and 3 mm superior, inferior, nasal, and temporal to the fovea. The numbers of eyes with measurable scleral thickness are shown in parentheses. Staphyloma, posterior staphyloma associated with pathologic myopia.

* $P < 0.01$.

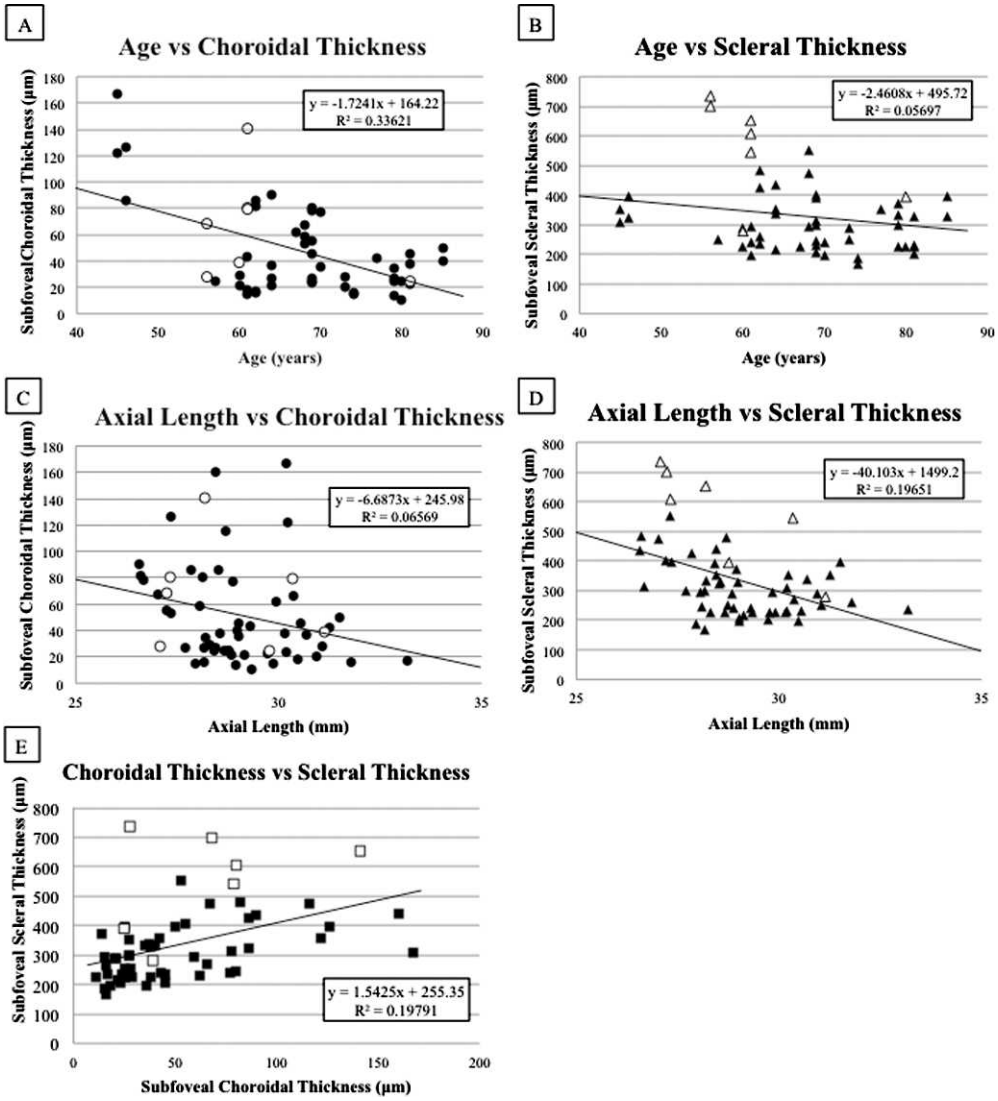

Figure 4. The graphs show the correlations between age and choroidal/scleral thickness (**A**, **B**), axial length and choroidal/scleral thickness (**C**, **D**), and choroidal and scleral thicknesses (**E**) in eyes with pathologic myopia. *Open circles* (**A**, **C**), *open triangles* (**B**, **D**), and *open squares* (**E**) indicate the eyes with a dome-shaped macula.

equation used was:

$$\textit{subfoveal scleral thickness} = 1237 - 0.37 \times \textit{age} - 32.3 \times \textit{AL} + 1.2 \times \textit{subfoveal choroidal thickness}$$

Multiple regression analysis showed that the subfoveal scleral thickness was well determined by the choroidal thickness and AL; however, the coefficient of determination was moderate ($R = 0.561$, $R^2 = 0.314$).

Table 2. Multiple Linear Regression Analyses for Scleral Thickness by Age, AL, and Choroidal Thickness

Factor	Coefficient	*P* Value	SE
Age (y)	−0.37	0.8	1.44
AL (mm)	−32.3	<0.01	10.67
Choroidal thickness (μm)	1.15	0.03	0.5
Intercept	1236.96	<0.01	349.48

SE, spherical equivalent.
$R = 0.561$, $R^2 = 0.314$.

Discussion

In our study, we measured the choroidal and scleral thicknesses in highly myopic eyes at the posterior pole using HP-OCT. Although the subfoveal sclera was the thickest compared with 3 mm outside of the fovea in eyes with a dome-shaped macula, even the subfoveal sclera without a dome-shaped macula was thicker than 3 mm outside of the fovea except around the peripapillary area. The AL and subfoveal choroidal thickness mostly seemed to affect the subfoveal scleral thickness.

A prior histopathologic study reported that the scleral thickness in normal eyes was approximately 0.9 to 1.0 mm around the posterior pole and approximately 0.4 mm around the equator. [1] A figure in that study showed that when the scleral thicknesses at each location were compared, the scleral thickness 3 mm temporal to the fovea was approximately 0.8 mm. In our results in highly myopic eyes using HP-OCT, the subfoveal scleral thickness was approximately 0.3 mm. Our results indicated that the subfoveal scleral thickness in eyes with an AL exceeding 26.5 mm was almost one-third of that in normal subjects (see comparison of Figs. 1–3). However, the subfoveal choroidal thicknesses in the highly myopic eyes in

our study (52 ± 38 μm) measured using HP-OCT and in a previous study (93 ± 63 μm) measured using EDI-OCT[3] also were thinner than normal, indicating that choroid and sclera were thinner due to ocular expansion.

Light and electron microscopy studies also have reported scleral abnormalities.[1,15–17] Severe scleral thinning is explained histopathologically as narrowing and dissociation of the collagen fiber bundles on light microscopy, and as diminished lamellar architecture of the fiber bundles, reduced diameter of the collagen fibrils, and loss of striations on electron microscopy. These alterations occur because of abnormal scleral stretching resulting from intraocular pressure changes. In our study, we observed the full-thickness sclera in all eyes and orbital fat in some eyes. The transparency increment might cause thinning and hollowing of abnormal scleral tissue in highly myopic eyes. In addition, the risk factors for myopia other than scleral abnormalities are thought to be environmental or genetic factors. Recently, genome-wide association studies identified a suspicious locus for myopia.[18,19]

However, the sclera did not become thinner homogeneously in each portion associated with AL elongation. In our study, the choroidal and scleral thicknesses with posterior staphyloma were significantly thinner than without posterior staphyloma. This might mean the scleral thickness was thinning within the posterior staphyloma. Also, the subfoveal sclera was significantly thicker than 3 mm outside the fovea. Even if a dome-shaped macula was excluded, the sclera at the subfoveal area and around the peripapillary area was thicker than at the other locations. These results might indicate that the sclera at the posterior pole in highly myopic eyes stretches inhomogeneously. Imamura et al. suggested that an adaptive mechanism might lead to a dome-shaped macula, that is the central macula remains focused on objects while the surrounding areas are relatively defocused.[13] Moreover, the surrounding area of defocus also is thought to extend the axial length and cause the myopia.[20–22] Thus, such an adaptive mechanism for defocusing may affect the progression of myopia even without a dome-shaped macula, and the subfoveal sclera might become thicker than other areas.

In conclusion, we evaluated and measured the choroid and the full-thickness sclera at the posterior pole in highly myopic eyes using HP-OCT. Especially, the AL and subfoveal choroidal thickness might affect the subfoveal scleral thickness according to the multiple regression equation. The sclera within the posterior pole was thickest at the subfoveal area and around the peripapillary area even in eyes without a dome-shaped macula. Although scleral thinning in highly myopic eyes was associated with scleral abnormalities, and environmental and genetic factors, the inhomogeneous scleral thickness at the posterior pole might be a protective mechanism to maintain focus and sharpness of vision around the fovea. Our study had several limitations, including its retrospective design, no follow-up, a small number of patients, and some missing data, such as the nasal scleral thicknesses. However, to our knowledge, our study was the first to observe a thin sclera in highly myopic eyes using HP-OCT, and suggested the importance of measuring the scleral thickness to understand better the pathogenesis and progression of pathologic myopia. HP-OCT can evaluate noninvasively the morphologic status in pathologic myopia.

References

1. Olsen TW, Aaberg SY, Geroski DH, Edelhauser HF. Human sclera: thickness and surface area. *Am J Ophthalmol*. 1998; 125:237–241.
2. Spaide RF, Koizumi H, Pozzoni MC. Enhanced depth imaging spectral-domain optical coherence tomography. *Am J Ophthalmol*. 2008;146:496–500.
3. Fujiwara T, Imamura Y, Margolis R, Slakter JS, Spaide RF. Enhanced depth imaging optical coherence tomography of the choroid in highly myopic eyes. *Am J Ophthalmol*. 2009;148: 445–450.
4. Margolis R, Spaide RF. A pilot study of enhanced depth imaging optical coherence tomography of the choroid in normal eyes. *Am J Ophthalmol*. 2009;147:811–815.
5. Imamura Y, Fujiwara T, Margolis R, Spaide RF. Enhanced depth imaging optical coherence tomography of the choroid in central serous chorioretinopathy. *Retina*. 2009;29:1469–1473.
6. Maruko I, Iida T, Sugano Y, et al. Subfoveal choroidal thickness after treatment of Vogt-Koyanagi-Harada disease. *Retina*. 2011; 31:510–517.
7. Koizumi H, Yamagishi T, Yamazaki T, Kawasaki R, Kinoshita S. Subfoveal choroidal thickness in typical age-related macular degeneration and polypoidal choroidal vasculopathy. *Graefes Arch Clin Exp Ophthalmol*. 2011;249:1123–1128.
8. Ikuno Y, Maruko I, Yasuno Y, et al. Reproducibility of retinal and choroidal thickness measurements in enhanced depth imaging and high-penetration optical coherence tomography. *Invest Ophthalmol Vis Sci*. 2011;52:5536–5540.
9. Hirata M, Tsujikawa A, Matsumoto A, et al. Macular choroidal thickness and volume in normal subjects measured by swept-source optical coherence tomography. *Invest Ophthalmol Vis Sci*. 2011;52:4971–4978.
10. Agawa T, Miura M, Ikuno Y, et al. Choroidal thickness measurement in healthy Japanese subjects by three-dimensional high-penetration optical coherence tomography. *Graefes Arch Clin Exp Ophthalmol*. 2011;249:1485–1492.
11. Usui S, Ikuno Y, Miki A, Matsushita K, Yasuno Y, Nishida K. Evaluation of the choroidal thickness using high-penetration optical coherence tomography with long wavelength in highly myopic normal-tension glaucoma. *Am J Ophthalmol*. 2012; 153:10.e1–16.e1.
12. Ohno-Matsui K, Akiba M, Moriyama M, Ishibashi T, Tokoro T, Spaide RF. Imaging retrobulbar subarachnoid space around optic nerve by swept-source optical coherence tomography in eyes with pathologic myopia. *Invest Ophthalmol Vis Sci*. 2011;52:9644–9650.
13. Imamura Y, Iida T, Maruko I, Zweifel SA, Spaide RF. Enhanced depth imaging optical coherence tomography of the sclera in dome-shaped macula. *Am J Ophthalmol*. 2011;151:297–302.
14. Maruko I, Iida T, Sugano Y, Oyamada H, Sekiryu T. Morphologic choroidal and scleral changes at the macula in tilted disc syndrome with staphyloma using optical coherence tomography. *Invest Ophthalmol Vis Sci*. 2011;52:8763–8768.
15. Curtin BJ, Teng CC. Scleral changes in pathologic myopia. *Trans Am Acad Ophthalmol Otolaryngol*. 1957;62:777–788.
16. Curtin BJ, Iwamoto T, Renaldo DP. Normal and staphylomatous sclera of high myopia. An electron microscopic study. *Arch Ophthalmol*. 1979;97:912–915.
17. Grossniklaus HE, Green WR. Pathologic findings in pathologic myopia. *Retina*. 1992;12:127–133.
18. Solouki AM, Verhoeven VJ, van Duijn CM, et al. A genome-wide association study identifies a susceptibility locus for refractive errors and myopia at 15q14. *Nat Genet*. 2010;42:897–901.
19. Hysi PG, Young TL, Mackey DA, et al. A genome-wide association study for myopia and refractive error identifies a susceptibility locus at 15q25. *Nat Genet*. 2010;42:902–905.
20. Smith EL III, Hung LF, Huang J, Blasdel TL, Humbird TL, Bockhorst KH. Effects of optical defocus on refractive development in monkeys: evidence for local, regionally selective mechanisms. *Invest Ophthalmol Vis Sci*. 2010;51:3864–3873.
21. Read SA, Collins MJ, Sander BP. Human optical axial length and defocus. *Invest Ophthalmol Vis Sci*. 2010;51:6262–6269.
22. Rosén R, Lundström L, Unsbo P. Influence of optical defocus on peripheral vision. *Invest Ophthalmol Vis Sci*. 2011;52:318–323.